AIP Advances

Inducing strong magnetism in $Cr_{20}Mn_{20}Fe_{20}Co_{20}Ni_{20}$ high-entropy alloys by exploiting its anti-Invar property

Cite as: AIP Advances **9**, 095037 (2019); https://doi.org/10.1063/1.5120251
Submitted: 16 July 2019 . Accepted: 10 September 2019 . Published Online: 24 September 2019

M. Acet

Inducing strong magnetism in $Cr_{20}Mn_{20}Fe_{20}Co_{20}Ni_{20}$ high-entropy alloys by exploiting its anti-Invar property

Cite as: AIP Advances 9, 095037 (2019); doi: 10.1063/1.5120251
Submitted: 16 July 2019 • Accepted: 10 September 2019 •
Published Online: 24 September 2019

M. Acet[a)]

AFFILIATIONS

Experimentalphysik AG Farle, Universität Duisburg-Essen, D-47048 Duisburg, Germany

[a)]mehmet.acet@uni-due.de

ABSTRACT

The equiatomic high-entropy alloy $Cr_{20}Mn_{20}Fe_{20}Co_{20}Ni_{20}$ high-entropy alloy has a valence-electron-concentration of 8 electrons/atom which is equivalent to that of Fe. The alloy being FCC is therefore electronically equivalent to FCC-Fe. We show through the thermal expansion properties that the alloy carries similar anti-Invar properties as FCC-Fe, but unlike FCC-Fe it is stable throughout its solid-state temperature-range. Therefore, by exploiting the anti-Invar property and expanding the lattice of the alloy by introducing interstitial carbon, we make $Cr_{20}Mn_{20}Fe_{20}Co_{20}Ni_{20}$ ferromagnetic with a Curie temperature lying above room temperature.

Mixing numerous 3d-elements and subsequently melting them together or allowing them to undergo a solid-state reaction gives rise to random solid solutions with a high configurational entropy.[1–4] The classical example is the CrMnFeCoNi alloy with an equiatomic composition of a 20 at% forming a single FCC phase. It is paramagnetic at room temperature and has competing interactions at low temperatures.[5,6] This material has a valence electron concentration $(e/a) = 8$, which is the same as that for elemental Fe, but instead of being BCC at room temperature, it is FCC. FCC-Fe is an anti-Invar with the atomic binding having a strongly enhanced anharmonicity and is also essentially non-magnetic at small volumes and ferromagnetic (FM) at expanded volumes.[7,8] We show here first that FCC CrMnFeCoNi is also an anti-Invar similar to FCC-Fe. Next, we expand the lattice of CrMnFeCoNi by introducing carbon to fill the octahedral sites of the FCC structure with 20 at% C. We thereby maintain $(e/a) = 8$, so that we have $(CrMnFeCoNi)_{80}C_{20}$. This becomes FM at room temperature with a Curie temperature $T_C = 400$ K and an average magnetic moment $\mu = 1.5\ \mu_B$; both with room to increase.

It is interesting that materials composed of 5-6 elements can exhibit a single uniform crystallographic phase despite competing structures of the individual elements. Such alloys, under the name of high-entropy, exhibit unsurpassed mechanical strength properties, and therefore, have been the focus of much research particularly in materials science.[9]

Although the material properties of these alloys have been widely covered and interest in further research is still maintained, their basic physical aspects have been largely overlooked. Some works on the magnetic properties can be found – which are mainly related to magnetic characterizations.[5,6,10–17] The nature of exchange interactions, discussing the antiferromagnetic exchange introduced by Cr and Mn in high entropy alloys have been introduced through magnetization studies on quaternary high entropy alloys[12] and quinternary alloys by Mössbauer studies.[18,19] When taken into account from a basic physical point of view however, equiatomic CrMnFeCoNi may be made to exhibit strong FM properties with Curie temperatures T_C lying well above room temperature. They may provide the possibility to attain magnetic moments that even exceed the Slater-Pauling rule. These can be realized by making use of the anti-Invar effect described briefly below.

Anti-invar systems (with FCC Fe as the prototype) have enhanced lattice anharmonicity extended out to larger volumes as compared to systems with regular lattice anharmonicity. The enhancement in the lattice anharmonicity is due to the presence of high-spin-states (HS) at non-equilibrium, expanded volumes

whereas the equilibrium ground state is a low-spin-state (LS). The magnetic moments μ in the ground state are 0.5 μ_B and 2.8 μ_B for the LS- and HS-states, respectively. With increasing temperature, the HS-state can be accessed through thermal magneto-volume fluctuations so that the lattice expansion of FCC-Fe becomes enhanced and can be written as

$$\alpha_{total}(T) = \alpha_{lattice}(T) + \alpha_{excess}(T), \quad (1)$$

where $\alpha_{total}(T)$ is the thermal expansion coefficient, $\alpha_{lattice}$ is the regular Grüneisen lattice contribution to the thermal expansion and α_{excess} is the excess contribution arising from HS-LS fluctuations.[8] $\alpha(T)$ for FCC-Fe is shown in Fig. 1.[20]

An overview of magnetic and structural properties of materials can be gained by examining a given physical parameter as a function of the material composition given in terms of the valence-electron-concentration (e/a). One of the earliest examples is the Slater-Pauling (SP) rule relating the average magnetic moment of 3d alloys and compounds to (e/a). The SP rule can go beyond as being a description of μ vs. e/a and can provide predictions of the magnetic moment of structures that are not stable under normal conditions. A sketch of the SP curve is given in Fig. 2 showing also an extrapolation of μ vs. e/a of the FCC regime to a structural regime where normally the BCC structure is stable; namely to (e/a) < 8.6. Here we see that if Fe or any other alloy, having (e/a) = 8, can been stabilized in the FCC structure in the HS-state at room temperature, it would have a magnetic moment $\mu \approx 2.8\ \mu_B$. This had been verified for FCC-Fe films.[21]

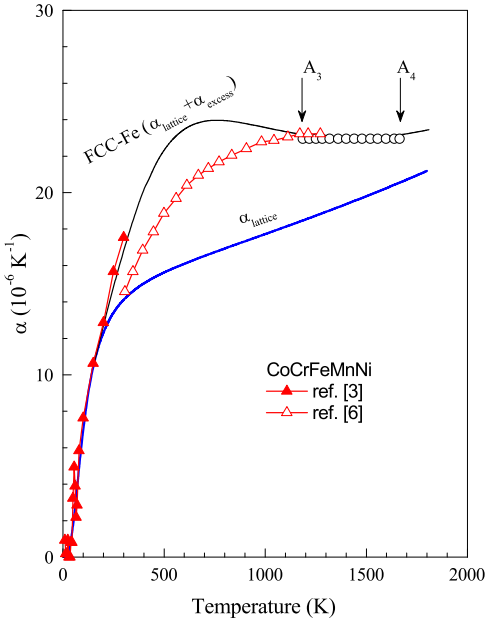

FIG. 1. A comparison of $\alpha(T)$ of FCC-Fe and the equielectronic alloy FCC-CrMnFeCoNi. FCC-Fe is stable between the A_3 and A_4 points. $\alpha_{lattice}$ denotes the Grüneisen expansion and is also representative for CrMnFeCoNi. As for FCC-Fe an excess lattice expansion is also seen for CrMnFeCoNi.

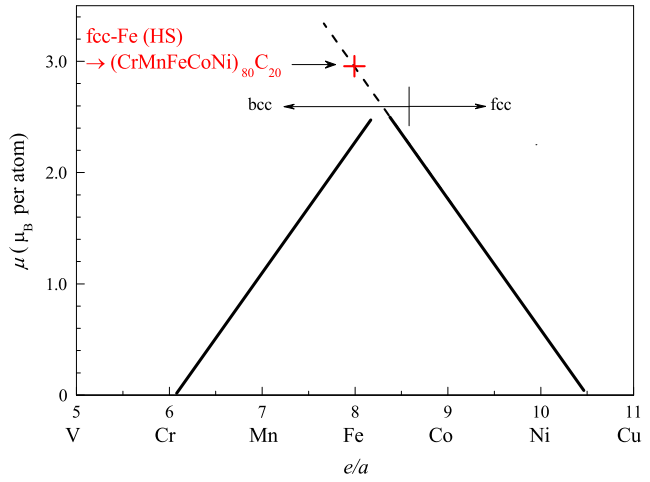

FIG. 2. A sketch of the Slater-Pauling rule giving the e/a-dependence of μ. The boundary between the BCC and FCC phases is at (e/a) ≈ 8.6. An extrapolation.

Since CrMnFeCoNi is FCC in the whole of the solid-state temperature-range, we ask whether this could have properties similar to those predicted for FCC Fe. Namely, since FCC-Fe is an anti-invar, could its isoelectronic counterpart CrMnFeCoNi also carry anti-Invar properties characterized with an enhanced $\alpha(T)$. $\alpha(T)$ calculated from the length-change data obtained for CrMnFeCoNi

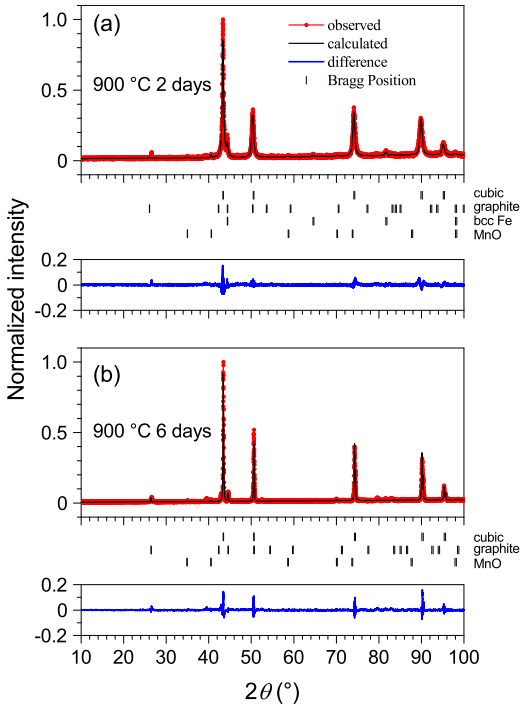

FIG. 3. XRD of $Cr_{16}Fe_{16}Mn_{16}Fe_{16}Co_{16}Ni_{16}C_{20}$ heat treated (a) at 900 °C for two days and (b) at 900 °C for 6 days.

in Refs. 3 and 6 and plotted in Fig. 1 shows that this alloy also has anti-invar properties with $\alpha(T)$ running well above $\alpha_{lattice}$ similar to $\alpha(T)$ of FCC-Fe. Therefore, CrMnFeCoNi shows anharmonically enhanced properties with the added virtue of being stable in the FCC-state at ambient temperatures and below. No considerable magnetic ordering is observed except for some frustration effects at low-temperatures arising from short-range ordering.[6] If such an anti-invar can be stabilized in the expanded-volume high-moment state, it can acquire long-range FM ordering.

Austenite is expanded FCC-Fe with a carbon atom 'squeezed' into the cube-octahedron. It is stable at temperatures above 700 °C. If carbon can be fitted similarly into the cube-octahedron of CrMnFeCoNi, it could be possible to introduce strong FM-exchange. To maintain $(e/a) = 8$ while introducing carbon we prepare $Cr_{16}Fe_{16}Mn_{16}Co_{16}Ni_{16}C_{20}$ by solid state reaction. 20 at% carbon ensures that all octahedral positions of the FCC structure are occupied by a carbon atom. The solid-state reaction was carried out by mixing powders of the elements, pressing them into pellets and firing them at 900 °C. Determining the exact carbon content by energy dispersive analysis is an issue. However, we can carry out a carbon-free estimation so that the relative stoichiometry of the resulting alloy is $Cr_{22}Mn_{21}Fe_{19}Co_{19}Ni_{19}$.

The refined x-ray diffraction (XRD) data obtained using Cu-K_α radiation is shown in Fig. 3. Fig. 3(a) shows the data for the sample annealed at 900 °C for two days. Patterns related to the FCC-CrMnFeCoNi, graphite BCC-Fe, and MnO are distinct and other phases with peaks of low-intensity are found. As the annealing time increases, the BCC-Fe-phase eventually disappears and the peaks related to graphite weaken as seen in Fig. 3(b). The peaks related to FCC-CrMnFeCoNi also become sharper. For a sample without carbon, we find the lattice parameter as 3.60 Å in agreement with earlier studies.[3,6] The results of the present refinements show that this increases to 3.62 Å when C is added corresponding to a lattice constant that would be the lattice constant of CrMnFeCoNi without carbon at 800 C. The major cubic phase being FCC and the increase of the lattice parameter are indications that carbon is introduced into interstitial positions. However, because of some remaining graphite and the off-stoichiometry, not all carbon is incorporated into the lattice.

We studied the change in the magnetic properties as the sample underwent various heat treatments. The sample cooled to 10 K in zero-field, and the field-dependence of the magnetization $M(B)$ was recorded. We show $M(B)$ in the range $-5 \le B \le 5$ T at 10 K in Fig. 4 with the sample annealed consecutively at 800 °C for 3 days, 900 °C for 2 days, and 900 °C for 6 days. Initially some remanence is observed which increases with increasing annealing-time and annealing-temperature. The saturation magnetization increases from 36.8 Am^2kg^{-1} when annealed at 800 °C to 52.7 Am^2kg^{-1} when annealed at 900 °C for 6 days. These values are still about five times lower than the expected saturation magnetization for $(e/a) = 8$ according to Fig. 2. $M(B)$ tends to saturation, however some high-field susceptibility remains due to the presence of non-FM components. In fact the presence of such components lead to a zero-field-cooled exchange bias caused by a field-induced spin-reconfiguration.[22]

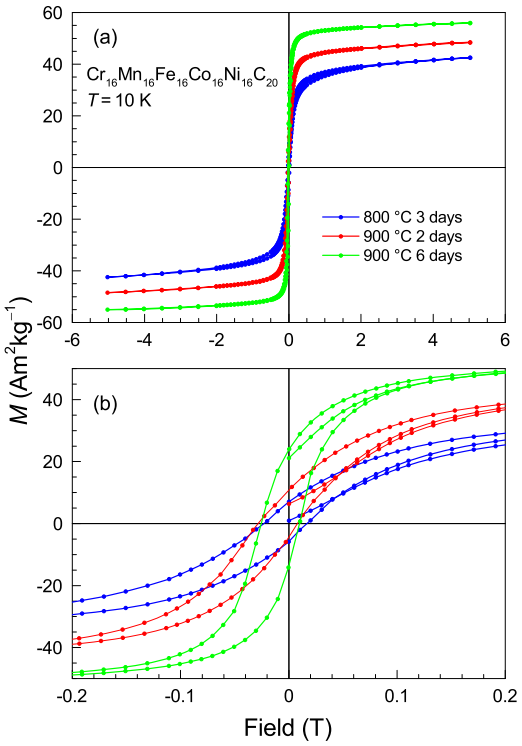

FIG. 4. $M(B)$ for $(CrMnFeCoNi)_{80}C_{20}$ for various annealing temperatures (a) measured in the range $-5 \le B \le 5$ T and (b) the details of the same data at low fields in the range $-0.2 \le B \le 0.2$ T.

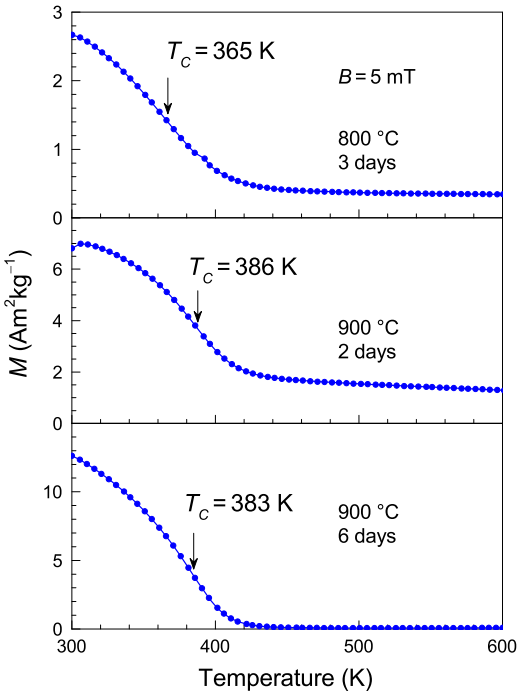

FIG. 5. $M(T)$ for $(CrMnFeCoNi)_{80}C_{20}$ for various annealing temperatures measured under 5 mT.

To determine the Curie temperature T_C, we measure the temperature-dependence of the magnetization $M(T)$ in a small field of 5 mT. We show $M(T)$ in Fig. 5 for the three annealing conditions. When measured in small fields, the magnetization at T_C should exhibit a sharp rise, after which it should run to lower temperatures at a constant value corresponding to the demagnetization limit. However, here we see that the transition to the FM state is smeared out over a broad temperature range indicating that the system is magnetically inhomogeneous with residual non-FM entities. Such smearing has been previously explained in terms of distributed exchange[23] as also suggested by the results of Mössbauer experiments, which evidence discrete exchange interactions.[19] Nevertheless a change in T_C can be observed from the figure. When annealed at 800 °C for 3 days T_C is about 365 K, whereas it increases to 386 K when annealed at 900 °C for a further 2 days. Thereafter, T_C does not change significantly.

In all cases, we find that by introducing C interstitially into CrMnFeCoNi causes a lattice expansion and leads to long-range ferromagnetic ordering with T_C above room temperature and a magnetization that tends to increase as the structure tends to stabilize at longer annealing-times and annealing-temperatures. An optimization of the carbon content can further increase both μ and T_C as well as introducing other interstitials such as nitrogen and boron. Therefore, exploiting the anti-Invar effect of high-entropy alloys can lead to new FM materials.

The author thanks M. Spasova for useful discussions.

REFERENCES

[1] J.-W. Yeh, S.-K. Chen, S.-J. Lin, J.-Y. Gan, T.-S. Chin, T.-T. Shun, C.-H. Tsau, and S.-Y. Chang, Adv. Eng. Mater. **6**, 299 (2004).
[2] Y. F. Ye, Q. Wang, J. Lu, C. T. Liu, and Y. Yang, Mater. Today **19**, 349 (2016).
[3] G. Laplanche, P. Gadaud, O. Horst, F. Otto, G. Eggeler, and E. P. George, J. Alloy. Comp. **623**, 348 (2015).
[4] D. B. Miracle and O. N. Senkov, Acta Mater. **122**, 448 (2017).
[5] Y. P. Wang, B. S. Li, and H. Z. Fu, Adv. Eng. Mater. **11**, 641 (2009).
[6] O. Schneeweiss, M. Friák, M. Dudová, D. Holec, M. Sob, D. Kriegner, V. Holý, P. Beran, E. P. George, J. Neugebauer, and A. Dlouhý, Phys. Rev. B **96**, 014437 (2017).
[7] V. L. Moruzzi, P. M. Marcus, and J. Kübler, Phys. Rev. B **39**, 6957 (1989).
[8] M. Acet, H. Zhres, E. F. Wassermann, and W. Pepperhoff, Phys. Rev. B **49**, 6012 (1994).
[9] B. Schuh, F. Mendez-Martin, B. Völker, E. P. George, H. Clemens, R. Pippan, and A. Hohenwarter, Acta Mater. **96**, 258 (2015).
[10] C.-Z. Yao, P. Zhang, M. Liu, G.-R. Li, J.-Q. Ye, P. Liu, and Y.-X. Tong, Electrochim. Acta **53**, 8359 (2008).
[11] Y. F. Kao, S.-K. Chen, T.-J. Chen, P. C. Chu, J. W. Yeh, and S.-J. Lin, J. Alloy. Compd. **509**, 1607 (2011).
[12] M. S. Lucas, L. Mauger, J. A. Munñoz, Y. Xiao, A. O. Sheets, S. L. Semiatin, J. Horwath, and Z. Turgut, J. Appl. Phys. **109**, 07E307 (2011).
[13] S. Singh, N. Wanderka, K. Kiefer, K. Siemensmeyer, and J. Banhart, Ultramicroscopy **111**, 619 (2011).
[14] Y. Zhang, T. T. Zuo, Y. Q. Cheng, and P. K. Liaw, Sci. Rep. **3**, 1455 (2013).
[15] M. S. Lucas, D. Belyea, C. Bauer, N. Bryant, E. Michel, Z. Turgut, S. O. Leontsev, J. Horwath, S. L. Semiatin, M. E. McHenry, and C. W. Miller, J. Appl. Phys. **113**, 17A923 (2013).
[16] C. Niu, A. J. Zaddach, A. A. Oni, X. Sang, J. W. Hurt III, J. M. LeBeau, C. C. Koch, and D. L. Irving, Appl. Phys. Lett. **106**, 161906 (2015).
[17] P. Li, W. Wang, and C. T. Liu, J. Alloy. Compd. **694**, 55 (2017).
[18] A. Perrin, M. Sorescu, M.-T. Burton, D. E. Laughlin, and M. E. McHenry, J. Materials **69**, 2125 (2017).
[19] A. Perrin, M. Sorescu, V. Ravi, D. E. Laughlin, and M. E. McHenry, AIP Advances **9**, 035329 (2019).
[20] W. Pepperhoff and M. Acet, *Constitution and Magnetism of Iron and its Alloys* (Springer-Verlag, Berlin, Heidelberg, 2001), p. 69.
[21] W. Keune, T. Ezawa, W. A. A. Macedo, U. Glos, K. P. Schletz, and U. Kirschbaum, Physica B **161**, 269 (1989).
[22] A. Cakir, M. Acet, and M. Farle, Phys. Rev. B **93**, 094411 (2016).
[23] N. J. Jones, H. Ucar, J. J. Ipus, M. E. McHenry, and D. E. Laughlin, J. Appl. Phys. **111**, 07A334 (2012).

DOI: 10.1063/1.5120251
URN: urn:nbn:de:hbz:464-20191203-130946-6